Respiratory Physiology & Neurobiology 183 (2012) 85–90

Contents lists available at SciVerse ScienceDirect

Respiratory Physiology & Neurobiology

journal homepage: www.elsevier.com/locate/resphysiol

Quantifying parenchymal tethering in a finite element simulation of a human lung slice under bronchoconstriction

Barbara J. Breen[a,*], Graham M. Donovan[b], James Sneyd[b], Merryn H. Tawhai[a]

[a] Auckland Bioengineering Institute, University of Auckland, Private Bag 92019 Auckland Mail Centre, Auckland 1142, New Zealand
[b] Department of Mathematics, University of Auckland, Private Bag 92019 Auckland Mail Centre, Auckland 1142, New Zealand

ARTICLE INFO

Article history:
Received 3 March 2012
Received in revised form 12 June 2012
Accepted 12 June 2012

Keywords:
Parenchymal tethering
Airway/parenchymal interaction
Computational modelling
Finite element modelling
Bronchoconstriction

ABSTRACT

Airway hyper-responsiveness (AHR), a hallmark of asthma, is a highly complex phenomenon characterised by multiple processes manifesting over a large range of length and time scales. Multiscale computational models have been derived to embody the experimental understanding of AHR. While current models differ in their derivation, a common assumption is that the increase in parenchymal tethering pressure P_{teth} during airway constriction can be described using the model proposed by Lai-Fook (1979), which is based on intact lung experimental data for elastic moduli over a range of inflation pressures. Here we reexamine this relationship for consistency with a nonlinear elastic material law that has been parameterised to the pressure–volume behaviour of the intact lung. We show that the nonlinear law and Lai-Fook's relationship are consistent for small constrictions, but diverge when the constriction becomes large.

1. Introduction

It is estimated that 300 million people worldwide suffer from asthma. According to the World Health Organization, this is expected to rise to 400 million by 2025, and almost 250,000 deaths per year are attributed to asthma (Bousquet et al., 2010). While evidence and theories implicate a variety of contributing factors from cellular to organ levels, asthma is perhaps best characterised as an emergent phenomena that is fundamentally a disease of airway constriction and obstruction. Constriction is usually categorised by response to agonist triggers. Airways that constrict too readily are hyper-sensitive; airways that contract too severely are hyper-responsive. Airway hyper-responsiveness (AHR) is of primary interest because it is associated with the majority of asthmatic mortality and morbidity (Sterk and Bel, 1989).

The lung tissue in which an airway is embedded can nontrivially modulate the rate at and degree to which the airway contracts. As the parenchyma is pulled inward with the airway wall during contraction, an increase in pressure in the parenchyma results from a tethering force that opposes contraction. This parenchymal tethering pressure arises from a combination of the elastic properties of structures in the lung tissue (generally attributed to collagen and elastin) and the alveolar surface tension.

It is well documented that the tethering pressure P_{teth} increases with increased lung volume (see, *e.g.*, An et al., 2007; Bates et al., 1994; Gunst et al., 1988; Okazawa et al., 1999). An asthmatic's inability to attenuate bronchoconstriction with a deep inspiration, for example, underscores the potential role of P_{teth} in the complex manifestation of airway hyper-responsiveness in asthma. All of these studies point to the importance of understanding the interdependence between airways and the lung parenchyma, both in asthmatics and in healthy subjects.

Computational models of airway contraction under bronchoconstriction that incorporate the effects of P_{teth} (*e.g.*, Anafi and Wilson, 2001; Khan et al., 2010; Politi et al., 2010) most commonly use the model proposed by Lai-Fook in 1979, which is based on seminal experiments correlating airway size and linear elastic moduli over a range of inflation pressures in intact dog lungs (Lai-Fook et al., 1976, 1978; Lai-Fook, 1979). These studies, although limited by technology available at the time, continue to be of value to today's models. The focus of the present study is to reexamine the Lai-Fook estimation for P_{teth} in light of current understanding of the nonlinear elastic material laws used to model the constitutive properties of experimentally unavailable tissue deep in the interior of the lung. The stress response of parenchyma to bronchoconstriction is simulated in a slice of lung tissue with nonlinear material properties. The development of tethering pressure is compared with the predictions of the Lai-Fook model under the same conditions.

2. Methods

A finite element (FE) model of a slice of lung tissue containing a cross-section of a terminal bronchiole is constructed using the

* Corresponding author. Tel.: +64 09 373 7599x84760; fax: +64 09 367 7157.
E-mail address: b.breen@auckland.ac.nz (B.J. Breen).

1569-9048/$ – see front matter © 2012 Elsevier B.V. All rights reserved.
http://dx.doi.org/10.1016/j.resp.2012.06.014

Table 1
Inflation pressures and resultant prestressed slice dimensions.

Volume	P_{init}	Area of slice	R_{init}
V_{ref}	0.0 cmH_2O	(3.0 mm)^2	0.200 mm
$V_1 = V_{FRC}$	3.9 cmH_2O	(3.8 mm)^2	0.252 mm
V_2	6.3 cmH_2O	(4.1 mm)^2	0.271 mm
V_3	9.1 cmH_2O	(4.3 mm)^2	0.286 mm
V_4	12.4 cmH_2O	(4.5 mm)^2	0.298 mm
V_5	17.4 cmH_2O	(4.7 mm)^2	0.310 mm
$V_6 = V_{TLC}$	24.8 cmH_2O	(4.8 mm)^2	0.321 mm

computational and visualisation software package CMISS (see Appendix A). The lung tissue is modelled as a compressible and nonlinearly elastic continuum with homogeneous and isotropic material properties (Fung, 1993; Kowalczyk and Kleiber, 1994; Tawhai et al., 2009).

The lung slice is created as a three-dimensional mesh composed of finite elements that are spatially located to produce the desired geometry of the slice, as shown in Fig. 1a. Eight nodes define each element and adjacent elements share nodes. The nonlinear elastic behaviour of the tissue is calculated at specific points in the mesh and interpolated between these points. Interpolation is accomplished using cubic Hermite basis functions (in each of the three coordinate directions) that enforce, at every node, continuity of all variables as well as of the first and second derivatives of variables. This higher-order interpolation method allows the slice geometry to be efficiently represented with fewer elements.

The "airway" is represented by a circular hole centred in the slice. The radius of the hole locates the boundary of the airway adventitia with the parenchyma, from which the tethering pressure arises. The model does not include any features of the airway itself: the smooth muscle layer, mucosal or epithelial layers, the basement membrane, *etc.*

The simulation and analysis focuses only on the stress that arises in the parenchyma as a result of being pulled inward with the contracting airway wall, *i.e.*, the hole that decreases in radius. The Cauchy stress, which represents the force per unit area of the deformed configuration (in units of cmH_2O), is calculated from the strain energy density function

$$W = ce^{(aJ_1^2 + bJ_2)}, \quad (1)$$

where J_1 and J_2 are the first and second invariants of the Green–Lagrangian finite strain tensor. The coefficients a, b and c do not have physical meaning. Their values were set to correlate with known elastic recoil pressures for uniform volume expansions in zero gravity (see Tawhai et al., 2009). Further details of the parameterisation of this model are included in Section 4.

From a reference state defined to have zero stress and zero strain, the tissue is prestressed to six different inflation pressures. The operational regime of the lung is far away from zero stress and zero strain, and the reference state is not likely to exist physically (Fung, 1975). The reference volume V_{ref} is a theoretical convenience for the mechanics problem and was set at half the functional residual capacity (FRC) volume, V_{FRC}. In combination with the parameterisation of the strain energy density function W, this gives pressure-volume behaviour that is consistent with the *in vivo* lung. Preliminary simulations characterised the spatial extent of the induced stress–strain. The dimensions of the reference configuration, 3 mm × 3 mm × 0.2 mm, were then chosen to ensure that the simulated radial deformations do not generate effects influenced by the stationary perimeter, as shown in Fig. 1b. The radius of the hole in the reference configuration is 0.2 mm.

See Table 1 for the inflation pressures and resulting dimensional changes in the model. An inflation pressure of 3.9 cmH_2O corresponds to V_{FRC} and an inflation pressure of 24.8 cmH_2O corresponds to the total lung capacity (TLC) volume, V_{TLC}.

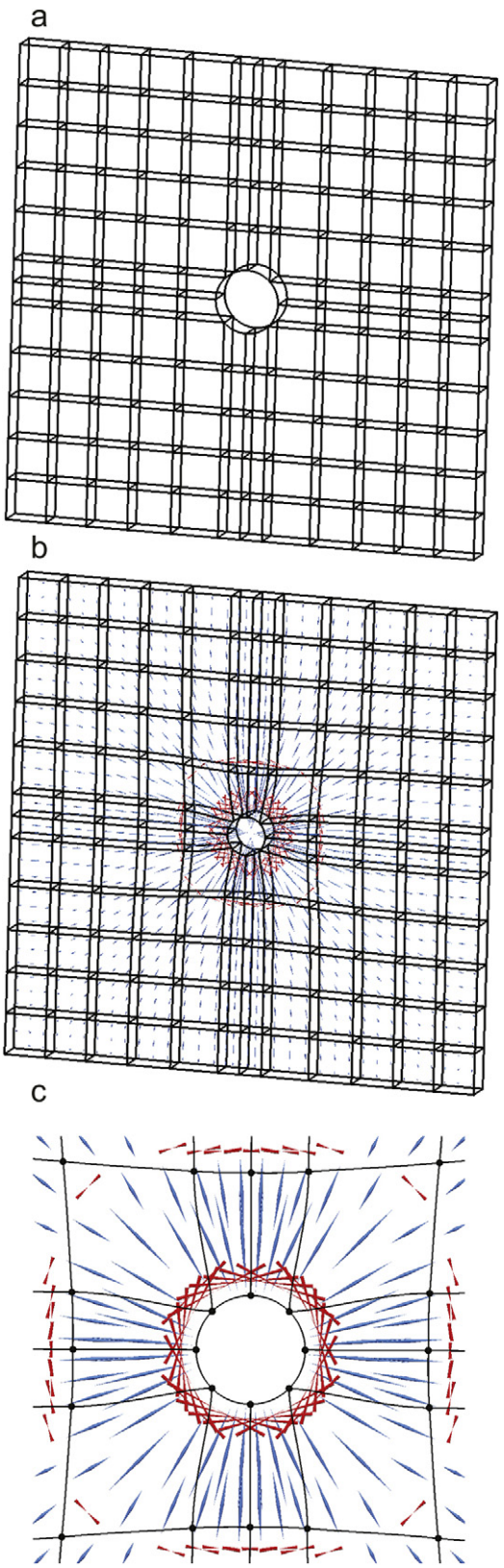

Fig. 1. Finite element model of lung slice with isolated airway. Panel (a) depicts starting configuration of the model, panel (b) shows the radial (blue) and circumferential (red) principal strains resulting from the simulated deformation and panel (c) is a close-up of the constricted airway at 60% R_{init}. (For interpretation of the references to color in this figure legend, the reader is referred to the web version of the article.)

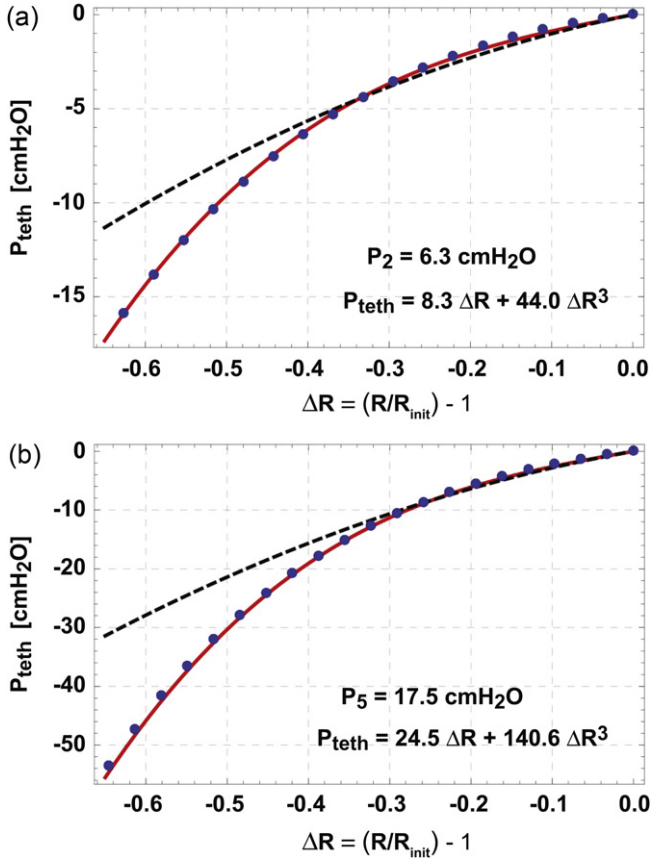

Fig. 2. Simulated effects of the tethering force on changes in transmural pressure, P_{teth} as a function of constricting radius, ΔR. Data is shown for two typical inflation pressures, (a) $P_2 = 6.3\,cmH_2O$ and (b) $P_5 = 17.5\,cmH_2O$. Dashed line (black) is P_{teth} predicted by Lai-Fook, Eq. (6). Disks (blue) are data from our slice simulation using nonlinear elastic material law. Solid line (red) is a cubic fit to our data. See Supplemental material for additional results. (For interpretation of the references to color in this figure legend, the reader is referred to the web version of the article.)

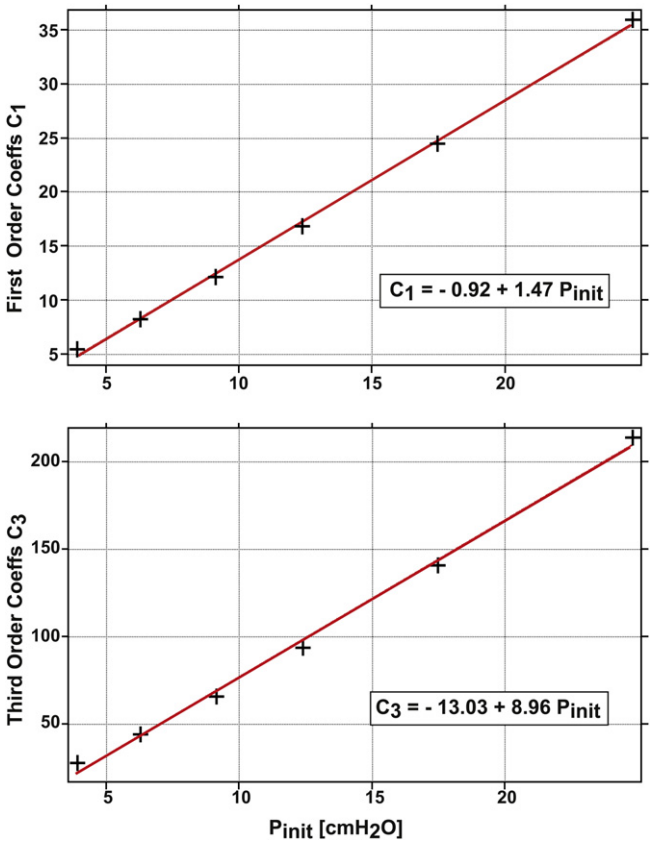

Fig. 3. Linear equations in P_{init} for P_{teth} fit coefficients C_1 and C_3. See Supplemental material for more detail.

After inflation, the outer dimensions of the slice are fixed. A series of quasi-static displacements are then enforced that decrease the airway radius to approximately 35% of its inflated value, R_{init}. Nodes on the perimeter of the airway are forced to move stepwise to decrease the airway radius symmetrically and the derivatives are unchanged to maintain circularity. All other internal nodes are free to move in response. Fig. 1c shows a close-up of an airway constricted to 60% R_{init}. The Cauchy stress resulting from the distortion of the FE grid is calculated at points evenly spaced around the hole. Only the stress in the tissue that ensues from the radial contraction is considered. To compare with results of the Lai-Fook experiments, the tethering pressure is defined to be the change in adventitial stress, $P_{teth} = P_{init} - P = \Delta P$, as the radius decreases. In analysis, its functional relationship to the dimensionless ratio of the change in radius R is found, where $\Delta R = (R - R_{init})/R_{init} = (R/R_{init}) - 1$.

3. Results

Data for two inflation pressures, $P_2 = 6.3\,cmH_2O$ and $P_5 = 17.5\,cmH_2O$, is shown in Fig. 2. The Lai-Fook model for the contribution of the tethering force to changes in the transmural pressure across the airway wall, $\Delta P = P_{teth}$ *vs.* ΔR, is shown as a dashed line in both panels. Lai-Fook characterised P_{teth} *vs.* ΔR as a quadratic equation referenced to the change in radius of the airway and to the shear modulus μ of the surrounding tissue,

$$P_{teth} = 2\mu(\Delta R + \alpha \Delta R^2), \tag{2}$$

where μ is a linear function of the transpulmonary pressure P_{TP} measured in a series of experiments and $\alpha = -1.5$ is a quadratic fit coefficient (Lai-Fook et al., 1976; Lai-Fook, 1979).

Our data, represented by disks in Fig. 2, does not differ significantly from the Lai-Fook predictions for $\Delta R > -0.4$ ($t(11) = -0.02$, $p > 0.05$). This is true across a broad range of initial inflation pressures (shown in detail in the Supplemental material). For greater contractions of the airway, $-0.7 < \Delta R < -0.4$, our model predicts a much stronger tethering force. The results generated by the nonlinear elastic material law in our slice model are best characterised by a cubic function, shown as a solid line in Fig. 2.

A cubic fit function has four coefficients. Because both P_{teth} and ΔR have initial values of zero, the constant term (y-intercept) for all our fits is zero, regardless of inflation pressure. In all cases the coefficient of the quadratic term was sufficiently smaller than the others that it could be held to zero as well. The resulting cubic fits therefore have only two non-zero terms: linear and cubic coefficients C_1 and C_3,

$$P_{teth} = C_1 \Delta R + C_3 \Delta R^3. \tag{3}$$

Although for all these simulations $P_{teth}\,(t_0) = 0$, the maximum value of tethering pressure (at maximum contraction) varied by almost a factor of 10 between initial pressures $P_1 = 3.9\,cmH_2O$ ($P_{teth}\,(t_f) = -10.5\,cmH_2O$) and $P_6 = 24.8\,cmH_2O$ ($P_{teth}\,(t_f) = -94.0\,cmH_2O$). However, the relationship between tethering coefficients and P_{init} was found to be roughly linear, as shown in Fig. 3, with the relationships between P_{init} and the coefficients approximated as

$$C_1 = -0.92 + 1.47 P_{init}, \tag{4}$$

$$C_3 = -13.03 + 8.96 P_{init}. \tag{5}$$

Note that the Lai-Fook model in Eq. (2) includes the shear modulus μ of the surrounding tissue while our cubic function does not. The Lai-Fook formulation for shear modulus is itself linearly related to transpulmonary pressure P_{TP}. For young adult human lungs, Lai-Fook reported values of μ from 0.7 P_{TP} to 0.9 P_{TP} over the range $4 \leq P_{TP} \leq 16\,cmH_2O$ (Lai-Fook and Hyatt, 2000). The comparisons made with Lai-Fook in Fig. 2 used $\mu = 0.7\,P_{init}$ and $\alpha = -1.5$, so that Eq. (2) may be restated as

$$P_{teth} = P_{init}(1.4\Delta R - 2.1\Delta R^2). \quad (6)$$

The nonlinear elastic material law of Eq. (1) does not explicitly include μ, which is inherently a linear material property. The strain energy density function used in this simulation represents gross *in vivo* tissue behaviour. Analyses included in Tawhai et al. (2009) demonstrate consistency between this material law and the change in bulk and shear moduli with inflation.

Since neither the bulk modulus nor the shear modulus is used to calculate the elastic recoil pressure of the lung tissue, the analysis of the current simulations yields no specific functional relationship between the shear modulus and the increase in tethering pressure during airway constriction. The Lai-Fook description of tethering pressure, as formulated in Eq. (6), enables a direct comparison with the cubic form predicted by the current simulations.

To investigate the implications of the revised parenchymal tethering relationships, two versions of the multiscale model of airway hyper-responsiveness of Politi et al. (2010) were implemented. The mechanics of this model is based on the work of Fung et al. (1978), Lai-Fook (1979) and Lambert et al. (1982). The dynamics of airway smooth muscle decreasing airway diameter upon agonist challenge is based on Wang et al. (2008).

The original version of this model uses the shear modulus μ in its calculation of the Lai-Fook P_{teth}, as in Eq. (2). This is done by first linearising the strain tensor around the airway and then perturbing the local strain state to calculate μ as the second Lamé parameter (see Supplemental Material in Politi et al., 2010). It is dynamically updated during simulation so that μ is a function of the current value of the transmural pressure P_{tm} at each time step. For these simulations, luminal pressure was set to 0, so P_{tm} was literally the pressure outside the airway. To implement P_{teth} as described by Eqs. (3)–(5), the current value of P_{tm} is used to calculate coefficients C_1 and C_3 at each time step. Everything else in the simulation is left as in Politi et al. (2010).

Fig. 4 shows the results of a study of the change in airway radius under agonist challenge using these two versions of the Politi model. The dashed line shows the implementation of Lai-Fook's description of P_{teth} and the solid line shows the results using Eqs. (3)–(5).

As can be seen in Fig. 4, the two descriptions of P_{teth} are in close agreement for small constrictions. The increase in P_{teth} predicted by nonlinear elastic material law only emerges at large constrictions.

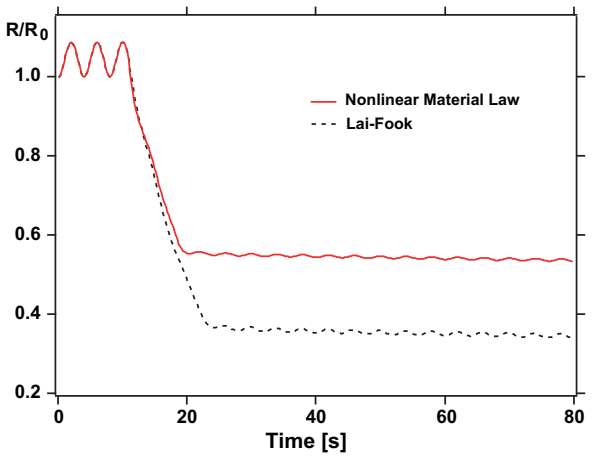

Fig. 4. An Order 1 airway during tidal breathing undergoes agonist challenge starting at $t = 10$ s. The radius is normalised to its initial value R_0. The dashed (black) curve incorporates the Lai-Fook model for P_{teth}. The solid (red) curve incorporates the model based on nonlinear elastic material law. (For interpretation of the references to color in this figure legend, the reader is referred to the web version of the article.)

4. Discussion

We have developed a new formulation for P_{teth} based on nonlinear elastic material law and compared this model to the Lai-Fook formulation that is currently in wide use. The whole lung intact tissue method of Lai-Fook and the Fung/Kowalczyk nonlinear elastic material law method employed in our model agree in what is essentially the linear regime, particularly where prestress pressures are moderate, *i.e.*, for $3.9 < P_{init} < 9.1\,cmH_2O$. We contend that the cubic nonlinearity is the more appropriate mathematical form to accommodate the nonlinear regime of parenchymal response, where it predicts stronger tethering pressures and smaller tissue compliance than Lai-Fook.

4.1. Historical context

In the late 1970s, Lai-Fook and others took the pragmatic approach of acquiring as much data as possible about the material behaviour of the lung from intact tissue. Using whole lungs of dogs, Lai-Fook derived values for the bulk and shear moduli in relation to the inflation pressure of the whole lung, and published his expression for tethering pressure in 1979. Follow-up studies showed that the linear relationship between shear modulus and P_{TP} remained consistent across species (Hajji et al., 1979). Lai-Fook and colleagues made measurements using a wick catheter on inflated ($\Delta R > 0$) blood vessels that supported the functional relationship between perivascular pressure and transpulmonary pressure in the intact canine lung (Goshy et al., 1979). Lai-Fook was also able to document age-related changes to the elastic moduli in human lungs (Lai-Fook and Hyatt, 2000).

Technological advancements have increased our understanding of the micromechanics of alveolar, vascular and pulmonary tissue structures, but not our ability to integrate this information into a coherent formulation of whole organ material properties. Thus Lai-Fook's work continues to be highly valued by the modelling community today, even while acknowledging that it provides no data about localised changes in the lung tissue.

In the absence of that data, Fung and others approached the question of lung tissue elasticity from the theoretical view of elastic material laws and derived a three-dimensional strain-energy function of the form seen in Eq. (1) (Fung et al., 1978; Lee and Frankus, 1975). Initially parameterised with experimental data from dog lungs and rabbit skin (Hoppin et al., 1975; Tong and Fung, 1976), the strain-energy formulation is under continual refinement. Human lung slice data was incorporated as available and applicable (Zeng et al., 1987), as was pseudoelasticity (Fung, 1993; Kowalczyk and Kleiber, 1994).

Since lung tissue is prestressed (there is no meaningful zero stress reference state *in vivo*), the theory of pseudoelasticity allows the stress–strain relationship for the lung to be separated into a loading and unloading branch, approximated as two hyperelastic materials, and the nonlinear elastic properties of each cycle are described *via* the coefficients of the strain energy density function, Eq. (1) (Fung, 1993). Finite element models of the whole lung such as Tawhai et al. (2009) are the direct descendants of this strategy.

What can clearly be seen in Fig. 2 is that the two approaches predict very similar values for P_{teth} for values of $\Delta R > -0.4$. They diverge significantly only for airway contractions where $-0.7 < \Delta R < -0.4$ and at higher prestress ($t(8) = -2.70$, $p < 0.05$) (see Supplemental material for detail). The whole lung intact tissue method of Lai-Fook and the Fung/Kowalczyk nonlinear elastic material law method agree in what is essentially the linear regime.

Considering the different approaches to understanding material properties of lung tissue that each represent, this is reassuring for both models. Lai-Fook's coefficients for his quadratic equation for tethering pressure were fit to $-0.4 < \Delta R < 0.15$ (Lai-Fook, 1979). Our study suggests that the Lai-Fook approximation is robust for small airway constrictions, but that it becomes less accurate for larger radial changes. The Lai-Fook approximation has its foundation in linear elasticity. The elastic constants provided by Lai-Fook and colleagues were from the beginning weakly characterised at high deformation and cannot be expected to be accurate in the nonlinear regime. The nonlinear material law suffers from weak parameterisation, yet it is entirely consistent with Lai-Fook's model over small deformations. This supports its appropriateness as an approximation to the nonlinear behaviour of intact tissue.

4.2. Model assumptions and limitations

The model features an extremely simplified anatomy: only a hole in the parenchyma is considered: the airway wall is not explicitly included. The contraction of the hypothetical airway is enforced quasi-statically, ignoring the dynamic effects of smooth muscle contraction, longitudinal shortening, or airway buckling. These simplifications allow a pure focus on the elastic recoil properties of the parenchyma. Longitudinal shortening may be significant in the intact lung – and should be addressed in future studies – however this is likely to be secondary to radial shortening. Of greater interest is the phenomenon of mucosal folding, which could introduce complex deformations adjacent to the airway wall. We maintained circularity at the parenchymal-airway interface, which is equivalent to the circularity that was maintained at the outer wall of the airway model proposed by Wiggs et al. (1997). A more complete analysis, and relaxation of the circularity constraint, would be achieved by combining these two types of models.

The strain energy density function used here lumps together the physical contributors to tissue tethering pressure. That is, the model does not differentiate between the contributions of tissue elasticity and surface tension to the parenchyma's elastic properties. Nor does it include independent alveolar, airway, and vascular components. The alveolar walls of the lung parenchyma have different elastic properties to the bronchial airway and vascular walls, which are generally assumed to be less compliant than the alveoli.

Our continuum material law is parameterised to whole intact lung, without consideration of distinct elastic properties of different tissue compartments. The model parenchyma that surrounds our contracting 'hole' is therefore representative of homogenised whole lung elastic behaviour – 'parenchymal tethering' is really 'tissue tethering' – which could conceivably differ from that of the parenchyma alone.

Lai-Fook's material law was similarly parameterised, as it was based on experiments from whole intact lung. Parameterisation to whole lung elasticity is therefore unlikely to cause differences between the two studies, however the inclusion of distinct elasticity for parenchyma and other structures could be important for improving the accuracy of this type of model analysis, and our understanding of the interplay between airway contraction and parenchymal tethering.

Ideally we would have used a material law that was specific to the parenchyma, *i.e.*, not homogenising the contributions of parenchyma, airways, and blood vessels. Data to parameterise such a material law is however currently not available.

The coefficients of the strain energy function were chosen such that uniform inflations to FRC and TLC required physiological pressures. The highly deformable elastic qualities of lung tissue distinguish it from all other biological tissue. Despite improvements in the technologies for soft tissue analysis, there is currently no good way to measure the constitutive properties of the lung, which emerge as a composite from the unique properties of a variety of structures: parenchymal, vascular and airway. Mathematical models of the lung are advanced by the combination of incremental experimental discovery, theoretical application and computer simulation. The best interpretation of the current state of whole-lung models is that they are weakly parameterised.

We do not intend our model to be compared directly with results from *ex vivo* lung slice experiments. *In vitro* validation of our results would require a protocol in which the alveolar mechanics was not disturbed by the experiment, and pressure could be measured at a fixed distance from the airway wall. We do not believe that *ex vivo* parenchymal 'slice' experiments are sufficient for this, as the alveolar configuration is disturbed by slicing and – in some studies – by agar filling the airspaces. It is not clear that the surface forces are similar to *in vivo.*

Comparison against *in vivo* data would also require localised pressure or force measurements, either at the airway wall or internal to the parenchyma. As we develop a better understanding of the relationship between airway size and force production in the airway smooth muscle, it could be possible to compare deformation in a 3D model that included the (active) airway wall against deformation of an intact airway-parenchymal system. However we are not aware of data that would currently facilitate this.

4.3. Future work

This slice model provides the opportunity to link nonlinear tethering pressures with dynamic radial changes caused by airway smooth muscle undergoing agonist challenge. We can continue to develop this FE model by incorporating the action of ASM under agonist challenge to dynamically contract the radius by crossbridge force and link these changes to the parenchyma.

Few continuum models incorporate both airway wall layers and the parenchyma. The tethering pressure formulation presented in this paper can be used as external boundary conditions for a finite element model of an isolated intact airway. Starting with, for example, an FE model of mucosal folding in a bi-layered airway where wall thickness can be varied (*e.g.*, Wiggs et al., 1997) a simulation can focus on the effect of the spiralling axial orientation of smooth muscle fibre, allowing axial length change while incorporating the effects of parenchymal tethering as algebraic functions of ΔR rather than in terms of the invariants of the strain tensor.

4.4. Concluding remarks

The increased magnitude of the tethering pressure at higher P_{tm} evokes its potential role as a contributing mechanism when deep inspirations attenuate bronchoconstriction in normal subjects (see, *e.g.*, Skloot et al., 1995). If, as LaPrad and Lutchen (2011) maintain, the lack of oscillatory mechanical strain does not cause AHR, the inability of an asthmatic patient to bronchodilate from a deep inspiration points to further consideration of reduced parenchymal tethering as a factor in airway hyper-responsiveness. We believe that our formulation for P_{teth} brings more accuracy as an initial condition for any investigation of the consequences of compromised parenchymal tethering.

The characteristics of the lung tissue/airway wall interaction play a non-trivial role in predicting airway contraction during

bronchoconstriction. The complexity of multiscale models demands of us a continuing effort to refine our understanding of the properties emerging from each scale. Models currently implementing tethering pressure as quadratic in the nonlinear regime may be underestimating the effects of parenchymal tethering.

Acknowledgement

This research was funded by NHLBI grant HL103405.

Appendix A. Soft tissue mechanics

CMISS (http://www.cmiss.org) is a computational and visualisation software package that provides a mathematical modelling environment for complex bioengineering problems. The strain energy density function that relates stress and strain in the lung tissue has been described in detail elsewhere, *e.g.*, Tawhai et al. (2009). Briefly, the lung is modelled as a homogeneous, compressible, nonlinearly elastic continuum. It is based on previous studies of lung tissue mechanics (Fung et al., 1978; Kowalczyk and Kleiber, 1994; Lambert et al., 1982), as well as on other soft tissues including human skin (Tong and Fung, 1976). Parameter values are set such that the model can be linked to CT measurements of human lungs. See *e.g.*, Burrowes and Tawhai (2010) and Tawhai et al. (2004, 2006).

The stress is calculated at 27 ($3 \times 3 \times 3$) spatially distributed Gauss points within each element. To record the change in pressure as the airway contracted, only Gauss points near the airway/parenchymal interface were used. The elastic recoil pressure P_{el} of the lung tissue increases with increasing volume, or equivalently, with increasing inflation pressure. At the boundary between the airway wall and the parenchyma, the tethering pressure P_{teth} that is acting on the outer surface of the airway wall must be equal and opposite to P_{el} acting internal to the parenchyma at that location.

Appendix B. Supplementary data

Supplementary data associated with this article can be found, in the online version, at http://dx.doi.org/10.1016/j.resp.2012.06.014.

References

An, S., Bai, T., Bates, J., Black, J., Brown, R., Brusasco, V., Chitano, P., Deng, L., Dowell, M., Eidelman, D., Fabry, B., Fairbank, N., Ford, L., Fredberg, J., Gerthoffer, W., Gilbert, S., Gosens, R., Gunst, S., Halayko, A., Ingram, R., Irvin, C., James, A., Janssen, L., King, G., Knight, D., Lauzon, A.M., Lakser, O., Ludwig, M., Lutchen, K., Maksym, G., Martin, J., Mauad, T., McParland, B., Mijailovich, S., Mitchell, H., Mitchell, R., Mitzner, W., Murphy, T., Paré, P., Pellegrino, R., Sanderson, M., Schellenberg, R., Seow, C., Silveira, P., Smith, P., Solway, J., Stephens, N., Sterk, P., Stewart, A., Tang, D., Tepper, R., Tran, T., Wang, L., 2007. Airway smooth muscle dynamics: a common pathway of airway obstruction in asthma. European Respiratory Journal 29, 834–860.

Anafi, R., Wilson, T., 2001. Airway stability and heterogeneity in the constricted lung. Journal of Applied Physiology 91, 1185–1192.

Bates, J., Lauzon, A.M., Dechman, G., Maksym, G., Schuessler, T., 1994. Temporal dynamics of pulmonary response to intravenous histamine in dogs: effects of dose and lung volume. Journal of Applied Physiology 76, 616–626.

Bousquet, J., Mantzouranis, E., Cruz, A., Aït-Khaled, N., Baena-Cagnani, C., Bleecker, E., Brightling, C., Burney, P., Bush, A., Busse, W., Casale, T., Chan-Yeung, M., Chen, R., Chowdhury, B., Chung, K., Dahl, R., Drazen, J., Fabbri, L., Holgate, S., Kauffmann, F., Haahtela, T., Khaltaev, N., Kiley, J., Masjedi, M., Mohammad, Y., O'Byrne, P., Partridge, M., Rabe, K., Togias, A., van Weel, C., Wenzel, S., Zhong, N., Zuberbier, T., 2010. Uniform definition of asthma severity, control, and exacerbations: document presented for the World Health Organization consultation on severe asthma. Journal of Allergy and Clinical Immunology 126, 926–938.

Burrowes, K., Tawhai, M., 2010. Coupling of lung tissue tethering force to fluid dynamics in the pulmonary circulation. International Journal for Numerical Methods in Biomedical Engineering 26, 862–875.

Fung, Y., 1975. Stress, deformation and atelectasis of the lung. Circulation Research 37, 481–496.

Fung, Y., 1993. Biomechanics: Mechanical Properties of Living Tissue, 2nd ed. Springer-Verlag, New York, Chapter 7.

Fung, Y., Tong, P., Patitucci, P., 1978. Stress and strain in the lung. Journal of the Engineering Mechanics Division 104, 201–223.

Goshy, M., Lai-Fook, S., Hyatt, R., 1979. Perivascular pressure measurements by wick-catheter technique in isolated dog lobes. Journal of Applied Physiology: Respiratory, Environmental and Exercise Physiology 46 (5), 950–955.

Gunst, S., Warner, D., Wilson, T., Hyatt, R., 1988. Parenchymal interdependence and airway response to methacholine in excised dog lobes. Journal of Applied Physiology 65 (6), 2490–2497.

Hajji, M., Wilson, T., Lai-Fook, S., 1979. Improved measurements of shear modulus and pleural membrane tension of the lung. Journal of Applied Physiology: Respiratory, Environmental and Exercise Physiology 47 (1), 175–181.

Hoppin Jr., F., Lee, G., Dawson, S., 1975. Properties of lung parenchyma in distortion. Journal of Applied Physiology 39 (5), 742–751.

Khan, M., Ellis, R., Inman, M., Bates, J., Sanderson, M., Janssen, L., 2010. Influence of airway wall stiffness and parenchymal tethering on the dynamics of bronchoconstriction. American Journal of Physiology – Lung Cellular and Molecular Physiology 299, L98–L108.

Kowalczyk, P., Kleiber, M., 1994. Modelling and numerical analysis of stresses and strains in the human lung including tissue–gas interaction. European Journal of Mechanics, A/Solids 13, 367–393.

Lai-Fook, S., 1979. A continuum mechanics analysis of pulmonary vascular interdependence in isolated dog lobes. Journal of Applied Physiology 46 (3), 419–429.

Lai-Fook, S., Hyatt, R., 2000. Effects of age on elastic moduli of human lungs. Journal of Applied Physiology 89, 163–168.

Lai-Fook, S., Hyatt, R., Rodarte, J., 1978. Effect of parenchymal shear modulus and lung volume on bronchial pressure-diameter behavior. Journal of Applied Physiology: Respiratory, Environmental and Exercise Physiology 44 (6), 859–868.

Lai-Fook, S., Wilson, T., Hyatt, R., Rodarte, J., 1976. Elastic constants of inflated lobes of dog lungs. Journal of Applied Physiology 40 (4), 508–513.

Lambert, R., Wilson, T., Hyatt, R., Rodarte, J., 1982. A computational model for expiratory flow. Journal of Applied Physiology: Respiratory, Environmental and Exercise Physiology 52 (1), 44–56.

LaPrad, A., Lutchen, K., 2011. The dissolution of intact airway responsiveness from breathing fluctuations: what went wrong? Journal of Applied Physiology 110, 1506–1507.

Lee, G., Frankus, A., 1975. Elasticity properties of lung parenchyma derived from experimental distortion data. Biophysical Journal 15, 481–493.

Okazawa, M., D'Yachkova, Y., Paré, P., 1999. Mechanical properties of lung parenchyma during bronchoconstriction. Journal of Applied Physiology 86, 496–502.

Politi, A., Donovan, G., Tawhai, M., Sanderson, M., Lauzon, A.M., Bates, J., Sneyd, J., 2010. A multiscale, spatially distributed model of asthmatic airway hyperresponsiveness. Journal of Theoretical Biology 266, 614–624.

Skloot, G., Permutt, S., Togias, A., 1995. Airway hyperresponsiveness in asthma: a problem of limited smooth muscle relaxation with inspiration. Journal of Clinical Investigation 96, 2393–2403.

Sterk, P., Bel, E., 1989. Bronchial hyperresponsiveness: the need for a distinction between hypersensitivity and excessive airway narrowing. European Respiratory Journal 2, 267–274.

Tawhai, M., Hunter, P., Tschirren, J., Reinhardt, J., McLennan, G., Hoffman, E., 2004. CT-based geometry analysis and finite element models of the human and ovine bronchial tree. Journal of Applied Physiology 97, 2310–2321.

Tawhai, M., Nash, M., Hoffman, E., 2006. An imaging-based computational approach to model ventilation distribution and soft-tissue deformation in the ovine lung. Academic Radiology 13, 113–120.

Tawhai, M., Nash, M., Lin, C.-L., Hoffman, E., 2009. Supine and prone differences in regional lung density and pleural pressure gradients in the human lung with constant shape. Journal of Applied Physiology 107, 912–920.

Tong, P., Fung, Y., 1976. The stress–strain relationship for the skin. Journal of Biomechanics 9, 649–657.

Wang, I., Politi, A., Bai, T., Sanderson, M., Sneyd, J., 2008. A mathematical model of airway and pulmonary arteriole smooth muscle. Biophysical Journal 94, 2053–2064.

Wiggs, B., Hrousis, C., Drazen, J., Kamm, R., 1997. On the mechanism of mucosal folding in normal and asthmatic airways. Journal of Applied Physiology 83, 1814–1821.

Zeng, Y., Yager, D., Fung, Y., 1987. Measurement of the mechanical properties of the human lung tissue. Journal of Biomechanical Engineering 109, 169–174.